with class B) (*14*, *17*, *18*). Consistent with a role for Cap-H2 in antagonizing homolog pairing, the $Ubx^{Cbx\text{-}1}$ $Ubx^{1}$/++ phenotype was dominantly enhanced by *Cap-H2* mutations [(Fig. 3A), compare class D with class E (Fig. 3C and table S1)]. Conversely, *Cap-H2* overexpression suppressed the $Ubx^{Cbx\text{-}1}$ $Ubx^{1}$/++ wing phenotype closer to wild-type [Fig. 3A, compare class D with class B (Fig. 3C and tables S3 to S5)].

*Cap-H2* mutant enhancement of the $Ubx^{Cbx\text{-}1}$ $Ubx^{1}$ phenotype was suppressed in a chromosomal rearrangement background [$R(Ubx^{Cbx\text{-}1}$ $Ubx^{1})$/++] that is thought to disrupt allelic associations between $Ubx^{Cbx\text{-}1}$ $Ubx^{1}$ and wild-type *Ubx* [(Fig. 3A), compare class E with class C (Fig. 3C, table S2)] (*7*). The $Ubx^{Cbx\text{-}1}$ $Ubx^{1}$/*Cap-H2*$^{-}$ and $R(Ubx^{Cbx\text{-}1}$ $Ubx^{1})$/*Cap-H2*$^{-}$ flies only vary by the reciprocal translocation that moves 3*R* bearing $Ubx^{Cbx\text{-}1}$ $Ubx^{1}$ to 2*R* and vice versa. This suggests that *Cap-H2* enhancement of the $Ubx^{Cbx\text{-}1}$ $Ubx^{1}$ phenotype is through increasing the association of homologous loci. Alternatively, Cap-H2 function may follow trans-chromosomal interactions, for example, acting locally to enable enhancer interactions in trans or as a general transcriptional repressor. Although either is formally possible, *Cap-H2*'s ability to globally disrupt aligned polytene structure suggests it carries out a related function in diploid cells to antagonize trans-chromosomal interactions.

Cap-H2 was tested in a second transvection system involving mutant alleles of the gene *yellow* (*y*). In $y^{82f29}/y^{82f29}$ and $y^{1\#8}/y^{1\#8}$ flies, there is minimal cuticle pigmentation, yet when placed in trans to one another ($y^{82f29}/y^{1\#8}$) complementation occurs with partial restoration of pigment nearer to wild-type levels. The $y^{1\#8}$ allele is a deletion of the *yellow* promoter and the $y^{82f29}$ allele a deletion of upstream enhancer elements. It is thought that partial complementation occurs in $y^{82f29}/y^{1\#8}$ through the ability of $y^{1\#8}$'s enhancers to act in trans, to associate with the intact promoter of $y^{82f29}$, and then to activate *yellow* transcription (*19*, *20*). As are $Ubx^{Cbx\text{-}1}$ $Ubx^{1}$, transvection of $y^{82f29}/y^{1\#8}$ is enhanced in a *Cap-H2* mutant background, which leads to darker pigmentation of the abdominal stripes relative to controls (Fig. 3, B and D) (*7*).

Transvection can be enhanced by slowing the rate of cell division (*21*). The percent of *Cap-H2* homozygous mutant cells specifically in mitosis was cytologically found to be greater relative to heterozygous controls, but this was statistically insignificant [1.37% ($n$ = 1318) versus 0.95% ($n$ = 3375), $P > 0.05$ ($\chi^2$)]. Furthermore, with flow cytometry, homozygotes and heterozygotes did not vary significantly in the percentage of cells in $G_1$, S, and $G_2$/M (fig. S12). Although these data do not rule out a cell cycle delay leading to enhanced transvection, they also do not support a major regulatory role for Cap-H2 in cell cycle progression. Cap-H2's ability to disassemble the aligned structure of polytene chromosomes instead suggests that it antagonizes transvection by inhibiting homology-dependent chromosomal interactions in diploid somatic cells.

Just as condensin-mediated supercoiling has been proposed to initiate chromosome condensation (*12*), we speculate that supercoiling activity also exists in interphase nuclei and can disrupt chromosome alignment. This may be through providing a force that physically disrupts interchromosomal associations and/or favors intrachromosomal higher-order structures that make inaccessible regions prone to trans-associate (fig. S13). This condensin activity may be a crucial aspect of gene regulation by disrupting trans-communication of allelic regulatory elements.

### References and Notes


1. I. W. Duncan, *Annu. Rev. Genet.* **36**, 521 (2002).
2. F. Savarese, R. Grosschedl, *Cell* **126**, 248 (2006).
3. F. Bantignies, C. Grimaud, S. Lavrov, M. Gabut, G. Cavalli, *Genes Dev.* **17**, 2406 (2003).
4. J. Vazquez, M. Muller, V. Pirrotta, J. W. Sedat, *Mol. Biol. Cell* **17**, 2158 (2006).
5. B. A. Edgar, T. L. Orr-Weaver, *Cell* **105**, 297 (2001).
6. K. J. Dej, A. C. Spradling, *Development* **126**, 293 (1999).
7. Materials and methods are available as supporting material on *Science* Online.
8. A. Schleiffer *et al*., *Mol. Cell* **11**, 571 (2003).
9. T. Hirano, *Curr. Biol.* **15**, R265 (2005).
10. T. Ono *et al*., *Cell* **115**, 109 (2003).
11. F. M. Yeong *et al*., *Curr. Biol.* **13**, 2058 (2003).
12. T. Hirano, *Nat. Rev. Mol. Cell Biol.* **7**, 311 (2006).
13. K. Kimura, T. Hirano, *Cell* **90**, 625 (1997).
14. E. B. Lewis, *Am. Nat.* **89**, 73 (1955).
15. C. V. Cabrera, J. Botas, A. Garcia-Bellido, *Nature* **318**, 569 (1985).
16. R. A. H. White, M. Akam, *Nature* **318**, 567 (1985).
17. J. E. Castelli-Gair, J. L. Micol, A. Garcia-Bellido, *Genetics* **126**, 177 (1990).
18. M. J. Gemkow, P. J. Verveer, D. J. Arndt-Jovin, *Development* **125**, 4541 (1998).
19. J. R. Morris, J. L. Chen, P. K. Geyer, C. T. Wu, *Proc. Natl. Acad. Sci. U.S.A.* **95**, 10740 (1998).
20. P. K. Geyer, M. M. Green, V. G. Corces, *EMBO J.* **9**, 2247 (1990).
21. M. M. Golic, K. G. Golic, *Genetics* **143**, 385 (1996).


22. We acknowledge T. Orr-Weaver for supporting the initial screen. We are grateful to the following individuals: C. Boswell (microscopy), V. Lien (UAS–Cap-H2–mCherry transgenics), M. Hart (mitotic index), P. Jansma (fly imaging), and J. Blumenstiel (FISH). We thank S. Hawley, T. Orr-Weaver, M. Lilly, E. Kelleher, and the JMST student forum for critical reading of the manuscript and, especially, C.-T. Wu for exceptional guidance with transvection studies. We are grateful to J. Sedat, J. Vazquez, C. Zuker, P. O'Farrell, and C.-T. Wu for fly stocks. Support was from NIH (GM069462) grant to G.B., and T.H. was funded by the University of Arizona NSF-IGERT (Integrative Graduate Education and Research Traineeships) Program in Genomics and NIH Grant for Graduate Training in Biochemistry and Molecular Biology.


### Supporting Online Material

www.sciencemag.org/cgi/content/full/322/5906/1384/DC1
Materials and Methods
SOM Text
Figs. S1 to S13
Tables S1 to S5
References
Movies S1 and S2

12 August 2008; accepted 2 October 2008
10.1126/science.1164216

# An Epigenetic Role for Maternally Inherited piRNAs in Transposon Silencing

**Julius Brennecke,[1]* Colin D. Malone,[1]* Alexei A. Aravin,[1] Ravi Sachidanandam,[1]† Alexander Stark,[2,3] Gregory J. Hannon[1]‡**

**In plants and mammals, small RNAs indirectly mediate epigenetic inheritance by specifying cytosine methylation. We found that small RNAs themselves serve as vectors for epigenetic information. Crosses between *Drosophila* strains that differ in the presence of a particular transposon can produce sterile progeny, a phenomenon called hybrid dysgenesis. This phenotype manifests itself only if the transposon is paternally inherited, suggesting maternal transmission of a factor that maintains fertility. In both *P*- and *I*-element–mediated hybrid dysgenesis models, daughters show a markedly different content of Piwi-interacting RNAs (piRNAs) targeting each element, depending on their parents of origin. Such differences persist from fertilization through adulthood. This indicates that maternally deposited piRNAs are important for mounting an effective silencing response and that a lack of maternal piRNA inheritance underlies hybrid dysgenesis.**

In *Drosophila melanogaster*, the progeny of intercrosses between wild-caught males and laboratory-strain females are sterile because of defects in gametogenesis, whereas the genetically identical progeny of wild-caught females and laboratory-strain males remain fertile (*1*–*3*). This phenomenon, known as hybrid dysgenesis, was attributed to the mobilization in dysgenic progeny of *P*-element or *I*-element transposons, which were present in wild-caught flies but absent from laboratory strains (*4*–*9*). The disparity in outcomes, depending on the parent of transposon origin, indicated the existence of cytoplasmically inherited determinants of the phenotype, which must be transmitted through the maternal germ line (*8*, *9*).

The control of mobile elements in germ cells depends heavily on a small RNA-based immune system, composed of Piwi-family proteins (Piwi, Aubergine, and AGO3) and piRNAs (*10*, *11*).

Both Piwi and Aubergine (Aub) are deposited into developing oocytes and accumulate in the pole plasm (*12*, *13*), implying possible transfer of maternal piRNAs into the germ lines of their progeny. We therefore asked whether maternally deposited small RNAs might affect transposon suppression in a heritable fashion and whether piRNAs might be the maternal suppressor of hybrid dysgenesis.

We first focused on *I*-element–induced hybrid dysgenesis (*14*). A cross of inducer males carrying active *I*-elements (designated "I" in Fig. 1) to reactive females devoid of active *I*-elements (designated "R") yielded dysgenic daughters (termed SF; Fig. 1 and fig. S1) (*5*, *6*, *8*, *15*). These were sterile, despite normal ovarian morphology. Sterility correlated with *I*-element expression in SF ovaries (Fig. 1B) (*16*). The reciprocal cross of inducer females to reactive males yielded fertile progeny (termed RSF; Fig. 1 and fig. S1).

[1]Watson School of Biological Sciences, Howard Hughes Medical Institute, Cold Spring Harbor Laboratory (CSHL), 1 Bungtown Road, Cold Spring Harbor, NY 11724, USA. [2]Broad Institute of Massachusetts Institute of Techonology and Harvard University, Cambridge, MA 02141, USA. [3]Computer Science and Artificial Intelligence Laboratory, Massachusetts Institute of Technology, Cambridge, MA 02139, USA.

*These authors contributed equally to this work.
†Present address: Department of Genetics and Genomic Sciences, Mount Sinai School of Medicine, New York, NY 10029, USA.
‡To whom correspondence should be addressed. E-mail: hannon@cshl.edu

We sequenced 18- to 29-nucleotide RNAs from the ovaries of inducer ($w^{1118}$) and reactive ($w^{k}$) strains, 0- to 2-hour embryos from dysgenic and nondysgenic crosses, and ovaries from SF and RSF daughters (Fig. 1A and fig. S1A). Both parental ovary and early embryo libraries contained similarly complex small RNA populations (fig. S1A). This indicates that small RNAs were maternally deposited, because the zygotic genome remains inactive during most of the period that we analyzed.

In *Drosophila*, piRNAs loaded into the Piwi, Aub, and AGO3 proteins exhibit distinctive features (*17*, *18*). piRNAs occupying Piwi and Aub are predominantly antisense to transposons and contain a 5′ terminal uridine residue (1U; fig. S2A). In contrast, AGO3 harbors mainly sense piRNAs with a strong bias for adenosine at position 10 (10A; fig. S2B). On the basis of these characteristics, we could infer the binding partner(s) for many small RNAs within our sequenced populations. A comparison of small RNAs in mothers and embryos indicated robust maternal inheritance for the Aub/Piwi pool and substantial but weaker deposition of AGO3-bound piRNAs (fig S2, A and B). This observation is consistent with the degree of maternal deposition of the corresponding Piwi-family proteins (figs. S3 and S4) (*12*, *13*).

Patterns of ovarian piRNAs targeting individual *D. melanogaster* transposons showed marked similarity between inducer and reactive strains (Fig. 2A). However, there were notable differences (Fig. 2, B and C). The *I*-element exhibited the lowest piRNA count in the reactive strain and the greatest disparity (21-fold) between strains (Fig. 2, B and C, and fig. S5A). Less pronounced differences were noted for *tirant* and *gypsy12*, which were more heavily targeted in the inducer strain, and for *1731* and *micropia*, which were more heavily targeted in the reactive strain (Fig. 2, B and C). These differences were mirrored in corresponding embryonic libraries, with reactive mothers depositing 12-fold fewer *I*-element piRNAs than inducer mothers (Fig. 2B). This supports the hypothesis that piRNAs correspond to the maternally transmitted phenotypic determinant noted in many studies of hybrid dysgenesis.

The outcome of an inducer-reactive (I-R) dysgenic cross manifests itself not in embryos but in adults. We therefore asked whether differences in maternally deposited piRNAs continued to influence adult piRNA profiles 2 weeks after fertilization. Consistent with their being genetically identical, SF and RSF daughters had virtually identical piRNA levels targeting nearly all transposons (Fig. 2, B and C). Thus, piRNA profiles for many elements had adjusted to a stable equilibrium during the course of germline development. As an example, for *1731* a ninefold difference in piRNA levels between mothers had equalized in progeny (fig. S5B). In RSF females, *I*-element piRNAs dropped twofold as compared

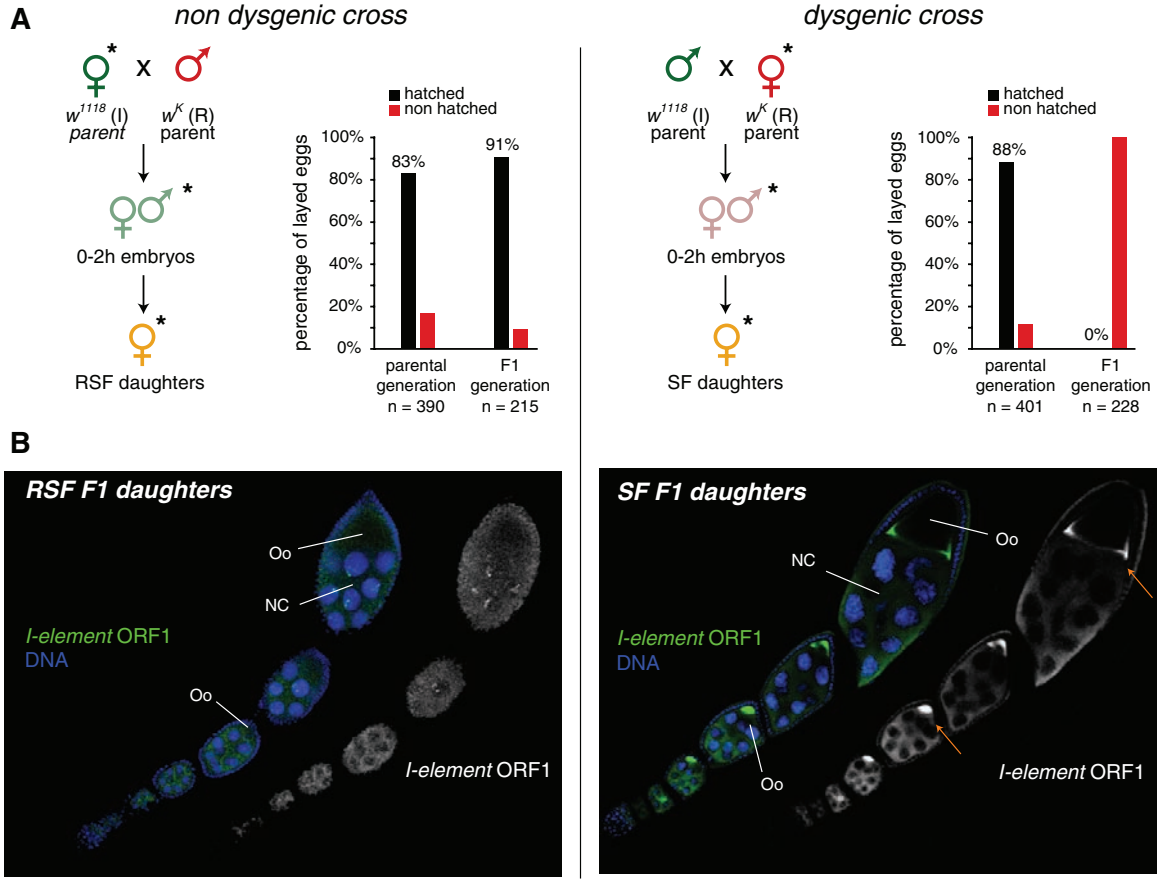


**Fig. 1.** The I-R hybrid dysgenesis system. (**A**) Crossing scheme to generate nondysgenic (left) and dysgenic (right) progeny. Small RNA libraries were made from flies indicated by asterisks. Bar diagrams indicate fertility analysis of parental and F1 females on the basis of egg hatching rates. *n*, number of counted eggs. (**B**) Immunofluorescence for *I*-element ORF1 (green) is shown for nondysgenic (RSF) and dysgenic (SF) daughters. Oo, oocyte; NC, nurse cells.

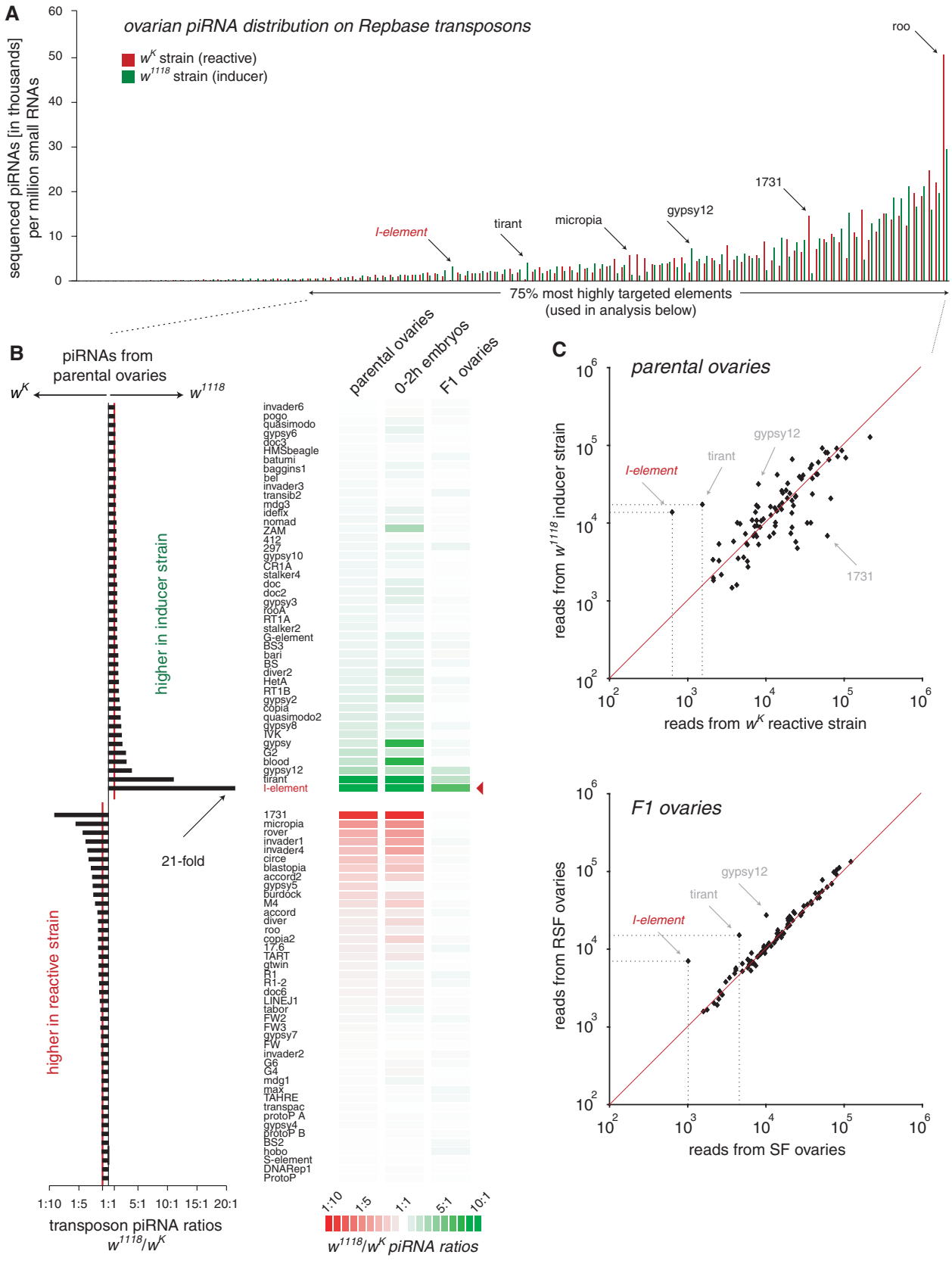


**Fig. 2.** I-R hybrid dysgenesis correlates with maternal piRNA inheritance. (**A**) Normalized piRNA counts for Repbase transposons are plotted for $w^{1118}$ inducer and $w^{K}$ reactive ovaries. (**B**) (Left) Fold differences in piRNA counts comparing $w^{1118}$ and $w^{K}$ mothers are shown (red line indicates a 1:1 ratio). (Right) Transposon piRNA ratios for mothers, embryos, and F1 progeny (SF: RSF ratio) are shown as a heat map. (**C**) Scatter plots indicating transposon piRNA correlations between $w^{1118}$ and $w^{K}$ mothers (top) and their respective intercross progeny (bottom).

with their inducer mothers (fig. S5B). This paralleled the overall reduction in active *I*-element load as the inducer genome was diluted by that of the reactive strain. However, limits on the adaptability of the system are seen in SF daughters for the *I*-element and, to a lesser degree, for *tirant* and *gypsy12* (Fig. 2, B and C, and fig. S5). Though SF daughters contained ~1.6-fold more *I*-element piRNAs than their reactive mothers, these were still sevenfold less abundant than in RSF daughters. This deficit ultimately results in de-repression of the paternally inherited, active *I*-elements and in sterility (Fig. 1, A and B).

Though active *I*-elements are confined to inducer strains, all *D. melanogaster* strains contain ancestral *I*-related fragments, (*6*, *19*–*21*). These are typically found in heterochromatin and exhibit 80 to 95% identity to the modern *I*-element. Such fragments have been proposed to mediate adaptation to and suppression of *I*-elements in inducer strains (*15*, *22*–*24*). To understand the lack of adaptation to *I*-elements in SF daughters, we probed the nature of interaction between active and ancestral *I*-element sequences.

The ping-pong model of piRNA biogenesis and silencing describes a Slicer-dependent amplification cycle between active transposons and

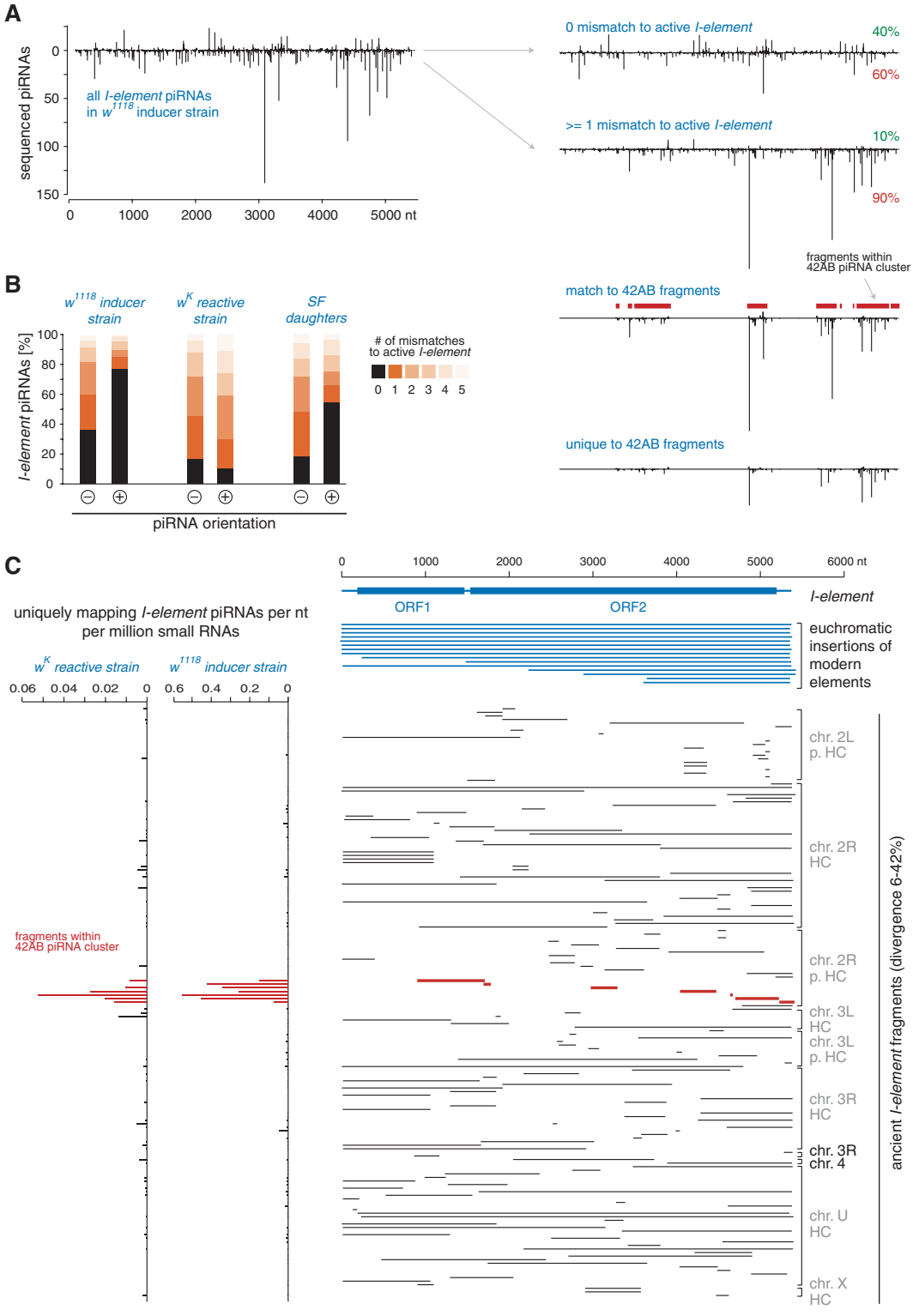


**Fig. 3.** A piRNA amplification loop between active *I*-elements and ancestral fragments. (**A**) Density profile of piRNAs matching the *I*-element with up to five mismatches (left) and profiles for those species with zero (top right) or at least one mismatch (below) to the active element (sense/antisense fractions in red and green) are shown. Profiles below indicate species that have the potential (upper) or must (lower) derive from the 42AB piRNA cluster. *I*-element fragments contained within the 42AB cluster are indicated in red. (**B**) Shown are fractions of *I*-element piRNAs from $w^{1118}$, $w^{K}$ mothers, and SF daughters (right) that match the active sequence with the indicated number of mismatches, split into sense (+) and antisense (–). (**C**) (Right) All *I*-element fragments in the Release 5 genome sequence [split into modern insertions (blue) and ancestral fragments (black) and sorted by chromosomal position] are shown (gray coloring indicates heterochromatic; HC, heterochromatin; p. HC, pericentromeric HC). Red fragments map to the 42AB piRNA cluster. (Left) Bar diagrams indicate the density of piRNAs mapping uniquely to the ancestral fragments shown at right (42AB fragments in red). As fragments with high piRNA density were not more divergent overall, clustering in 42AB is not an artifact of analysis (fig. S7).

transposon fragments resident in piRNA clusters (*17*, *18*). Sequence features fitting this model were obvious in piRNAs from the inducer strain (fig. S6). More than half of all *I*-element piRNAs deviated from the modern sequence and, therefore, must have originated from ancestral fragments (Fig. 3A). Of those piRNAs, the overwhelming majority (90%) were antisense. As a whole, sense-oriented species showed a strong tendency (~78%) to originate from modern active *I*-element copies (Fig. 3B), whereas 63% of antisense species must have originated from heterochromatic fragments.

Because the reactive strain lacks active *I*-element copies, no ping-pong amplification occurred, and piRNAs mapping to the sense or antisense strand showed no distinguishing pattern of matching to the active element (Fig. 3B). Despite the lack of an efficient silencing response in SF daughters, we still observed a clear trend for sense piRNAs to originate from active *I*-element copies, which were paternally transmitted (Fig. 3B). This is consistent with the adaptive system having begun to mount a response in SF daughters, although they ultimately failed to silence the element.

In both reactive and inducer strains, the 42AB cluster represents a major source of piRNAs targeting a variety of mobile elements (fig. S8) (*17*). Of all heterochromatic *I*-fragments present in the sequenced *melanogaster* strain, seven lie within 42AB, and we verified the existence of all in both our reactive and inducer strains (fig. S9). None of the other heterochromatic *I*-fragments lie within the remaining 19 most active clusters. In the inducer strain, the majority of heterochromatin-derived *I*-element piRNAs arose from ancestral fragments within 42AB, including many of the most abundant species (Fig. 3, A and C). Despite

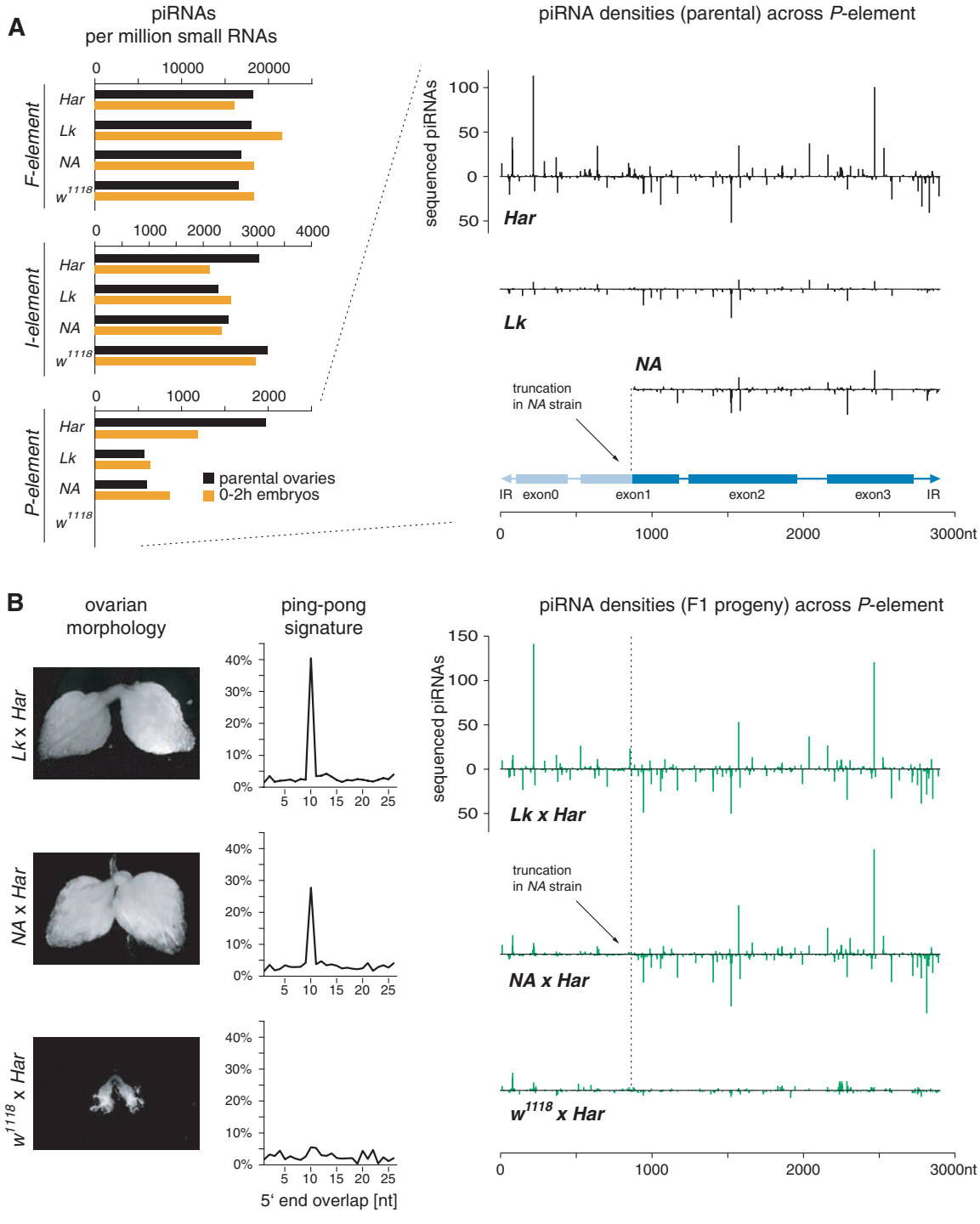


**Fig. 4.** Suppression of P-M hybrid dysgenesis correlates with maternally deposited piRNAs. (**A**) Normalized number of ovarian (black) and early embryonic (orange) piRNAs from the indicated strains mapping to the *F*-, *I*-, and *P*-elements with up to three (*F* and *I*) or with one (*P*) mismatch(es). To the right (sense, upper; antisense, lower), densities of piRNAs are displayed over the *P*-element in parental ovaries of the *Har*, *LK*, and *NA* strains. The extent of the truncation of the telomeric *P*-insertion in the *NA* strain is indicated. The intron-exon structure of the *P*-element is shown below. (**B**) F1 ovarian morphology, ping-pong signature, and piRNA densities from nondysgenic (*LK* × *Har* and *NA* × *Har*) and dysgenic ($w^{1118}$ × *Har*) F1 progeny are shown.

a more than 20-fold difference in their relative levels, *I*-element piRNAs matching heterochromatic fragments were also derived from 42AB in the reactive strain (Fig. 3C).

We sought to test whether the role of maternally inherited small RNAs in transposon silencing was general. In P-strain/M-strain (P-M) hybrid dysgenesis, crosses between males containing *P*-elements (P-strains) and females devoid of such elements (M-strains) yield sterile progeny with severe gonadal atrophy (GD sterility) (*3*, *9*). We examined small RNAs from *Harwich* (*Har*), a P-strain containing 30 to 50 *P*-element copies, and $w^{1118}$, here serving as an M-strain. *Harwich* showed strong maternal deposition of *P*-element piRNAs, whereas both M-strain mothers and their 0- to 2-hour embryos lacked such species (Fig. 4A). This contrasted with *I*- and *F*-element piRNAs, which were abundant in parents and embryos from both strains. Crosses between *Harwich* males and $w^{1118}$ females yielded dysgenic (GD) progeny. Because of the impact of severe gonadal atrophy (Fig. 4B and table S1), we normalized the daughter library using piRNAs targeting the *F*-element, a transposon exhibiting consistent profiles in all strains examined. Clearly, dysgenic daughters lacked prominent *P*-element piRNAs and signatures of the ping-pong amplification cycle (Fig. 4B).

*Lerik-P(1A)* (designated *Lk*) contains two *P*-elements in the X-TAS piRNA cluster, and *Nasr'Allah-P(1A)* (designated *NA*) contains a single 5′ truncated insertion at the same locus (*25*, *26*). *Lk* and *NA* both produce and maternally deposit *P*-element piRNAs (Fig. 4A), with these species in the *NA* strain precisely corresponding to the extent of its only *P*-fragment (Fig. 4A) (*25*). Unlike $w^{1118}$, *Lk* and *NA* mothers were able to produce fertile offspring with *Harwich*. This result correlated with robust piRNA production in daughter ovaries and with a strong signature of the ping-pong amplification cycle.

The 5′ end of the *P*-element largely lacked piRNAs, particularly antisense species, in both dysgenic flies and fertile *NA-Harwich* progeny (Fig. 4B). *NA* does not deposit maternal piRNAs corresponding to this region, because of the truncation of its *P*-element in X-TAS. Thus, maternal piRNAs are important for potent piRNA generation in daughters, even when the *P*-element is being effectively silenced by piRNAs matching other parts of the transposon.

piRNA clusters have been envisioned as a genetic reservoir of transposon resistance, with immunity being determined by the content of these loci (*17*). Our data indicate that the content of piRNA clusters alone is insufficient to provide resistance to at least some elements within a single generation. Instead, maternally inherited small RNAs appear to be essential to prime the resistance system at each generation to achieve full immunity (see also *27*).

In the I-R system, environmental factors influence the severity of the phenotype in a dysgenic cross (*28*) in a manner linked to the expression level of ancestral *I*-fragments (*29*). Rearing of reactive mothers at elevated temperature or increases in maternal age raise the proportion of fertile progeny. These observations suggest that the experience of the mother translates into a dominant effect on progeny. Our data suggest that this experience may be transmitted through variations in maternally deposited small RNA populations. Thus, transmission of instructive piRNA populations, shaped by both genetic and environmental factors, may provide a previously unknown mechanism for epigenetic inheritance.

### References and Notes


1. G. Picard, P. L'Heritier, *Drosophila Inf. Serv.* **46**, 54 (1971).
2. G. Picard, *Genetics* **83**, 107 (1976).
3. M. G. Kidwell, J. F. Kidwell, J. A. Sved, *Genetics* **86**, 813 (1977).
4. G. M. Rubin, M. G. Kidwell, P. M. Bingham, *Cell* **29**, 987 (1982).
5. A. Pelisson, *Mol. Gen. Genet.* **183**, 123 (1981).
6. A. Bucheton, R. Paro, H. M. Sang, A. Pelisson, D. J. Finnegan, *Cell* **38**, 153 (1984).
7. M. G. Kidwell, *Proc. Natl. Acad. Sci. U.S.A.* **80**, 1655 (1983).
8. S. Chambeyron, A. Bucheton, *Cytogenet. Genome Res.* **110**, 215 (2005).
9. J. P. Castro, C. M. Carareto, *Genetica* **121**, 107 (2004).
10. A. A. Aravin, G. J. Hannon, J. Brennecke, *Science* **318**, 761 (2007).
11. C. Klattenhoff, W. Theurkauf, *Development* **135**, 3 (2008).
12. H. B. Megosh, D. N. Cox, C. Campbell, H. Lin, *Curr. Biol.* **16**, 1884 (2006).
13. A. N. Harris, P. M. Macdonald, *Development* **128**, 2823 (2001).
14. Materials and methods are available as supporting material on *Science* Online.
15. S. Jensen, L. Cavarec, M. P. Gassama, T. Heidmann, *Mol. Gen. Genet.* **248**, 381 (1995).
16. M. C. Seleme, I. Busseau, S. Malinsky, A. Bucheton, D. Teninges, *Genetics* **151**, 761 (1999).
17. J. Brennecke *et al.*, *Cell* **128**, 1089 (2007).
18. L. S. Gunawardane *et al.*, *Science* **315**, 1587 (2007), published online 21 February 2007 (10.1126/science.1140494).
19. P. Dimitri, A. Bucheton, *Cytogenet. Genome Res.* **110**, 160 (2005).
20. M. Crozatier, C. Vaury, I. Busseau, A. Pelisson, A. Bucheton, *Nucleic Acids Res.* **16**, 9199 (1988).
21. C. Vaury, P. Abad, A. Pelisson, A. Lenoir, A. Bucheton, *J. Mol. Evol.* **31**, 424 (1990).
22. S. Jensen, M. P. Gassama, X. Dramard, T. Heidmann, *Genetics* **162**, 1197 (2002).
23. S. Jensen, M. P. Gassama, T. Heidmann, *Nat. Genet.* **21**, 209 (1999).
24. S. Malinsky, A. Bucheton, I. Busseau, *Genetics* **156**, 1147 (2000).
25. L. Marin *et al.*, *Genetics* **155**, 1841 (2000).
26. S. Ronsseray, M. Lehmann, D. Anxolabehere, *Genetics* **129**, 501 (1991).
27. J. P. Blumenstiel, D. L. Hartl, *Proc. Natl. Acad. Sci. U.S.A.* **102**, 15965 (2005).
28. A. Bucheton, *Heredity* **41**, 357 (1978).
29. X. Dramard, T. Heidmann, S. Jensen, *PLoS One* **2**, e304 (2007).


30. We thank M. Rooks and D. McCombie (CSHL) for help with deep sequencing, S. Jensen and S. Ronsseray for fly stocks and helpful discussions, and D. Finnegan for the *I*-element ORF-1 antibody. J.B. is supported by a fellowship from The Ernst Schering Foundation, C.D.M. is a Beckman fellow of the Watson School of Biological Sciences and is supported by an NSF Graduate Research Fellowship, and A.S. is supported by a Human Frontier Science Program fellowship. This work was supported by grants from NIH to G.J.H. and A.A.A. and a kind gift from K. W. Davis (to G.J.H.). Small RNA libraries are deposited at Gene Expression Omnibus (accession no. GSE13081, data sets GSM327620 to GSM327634).


### Supporting Online Material

www.sciencemag.org/cgi/content/full/322/5906/1387/DC1
Materials and Methods
Figs. S1 to S9
Tables S1 to S3
References

26 August 2008; accepted 27 October 2008
10.1126/science.1165171

# PA-824 Kills Nonreplicating *Mycobacterium tuberculosis* by Intracellular NO Release

**Ramandeep Singh,[1]* Ujjini Manjunatha,[1,2]* Helena I. M. Boshoff,[1] Young Hwan Ha,[1] Pornwaratt Niyomrattanakit,[2] Richard Ledwidge,[1] Cynthia S. Dowd,[1] Ill Young Lee,[1] Pilho Kim,[1] Liang Zhang,[1] Sunhee Kang,[1] Thomas H. Keller,[2] Jan Jiricek,[2] Clifton E. Barry 3rd[1]†**

**Bicyclic nitroimidazoles, including PA-824, are exciting candidates for the treatment of tuberculosis. These prodrugs require intracellular activation for their biological function. We found that Rv3547 is a deazaflavin-dependent nitroreductase (Ddn) that converts PA-824 into three primary metabolites; the major one is the corresponding des-nitroimidazole (des-nitro). When derivatives of PA-824 were used, the amount of des-nitro metabolite formed was highly correlated with anaerobic killing of *Mycobacterium tuberculosis* (Mtb). Des-nitro metabolite formation generated reactive nitrogen species, including nitric oxide (NO), which are the major effectors of the anaerobic activity of these compounds. Furthermore, NO scavengers protected the bacilli from the lethal effects of the drug. Thus, these compounds may act as intracellular NO donors and could augment a killing mechanism intrinsic to the innate immune system.**

Drug-resistant tuberculosis (TB) has emerged as a major threat to global health (*1*). Promising new candidate drugs are the bicyclic nitroimidazoles, including PA-824 and OPC-67683, which are currently in human clinical trials (*2*, *3*). These molecules are active not only against actively replicating bacteria, but also against bacteria that are nonreplicating by